

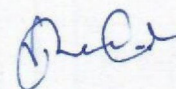
CERTIFICATE

It is certified that the work contained in the thesis titled "*Soft-Switching Modulation Techniques for Bidirectional Dual Active Bridge Converter Based Battery Charging Systems*" by *Priyatosh Jena* has been carried out under our supervision and that this work has not been submitted elsewhere for a degree.

It is further certified that the student has fulfilled all requirements of Comprehensive Examination, Candidacy, and SOTA for the award of Ph.D. Degree.



Prof. Rajeev Kumar Singh
Professor
Dept. of Electrical Engineering,
Indian Institute of Technology (BHU) Varanasi



Prof. Vivek Nandna Lal
Associate Professor
Dept. of Electrical Engineering,
Indian Institute of Technology (BHU) Varanasi

DECLARATION BY THE CANDIDATE

I, *Priyatosh Jena*, certify that the work embodied in this Ph.D. thesis is my own bonafide work carried out by me under the supervision of *Prof. Rajeev Kumar Singh* and co-supervision of *Prof. Vivek Nandan Lal* from *December 2019* to *March 2025* at *Department of Electrical Engineering*, Indian Institute of Technology (BHU) Varanasi. The matter embodied in this thesis has not been submitted for the award of any other degree/diploma. I declare that I have faithfully acknowledged and given credits to the research workers wherever their works have been cited in my work in this thesis. I further declare that I have not willfully copied any other's work, paragraphs, text, data, results, *etc.* reported in journals, books, magazines, reports, dissertations, theses, *etc.*, or available at websites and have not included them in this thesis and have not cited as my own work.

Date: 17-3-25

Place: Varanasi

Priyatosh Jena
Priyatosh Jena

CERTIFICATE BY THE SUPERVISOR

This is to certify that the above statement made by the candidate is correct to the best of our knowledge.

Rajeev Kumar Singh
17/3/25

Prof. Rajeev Kumar Singh

Professor

Dept. of Electrical Engineering,

Indian Institute of Technology (BHU) Varanasi

Vivek Nandan Lal

Prof. Vivek Nandan Lal

Associate Professor

Dept. of Electrical Engineering,

Indian Institute of Technology (BHU) Varanasi

Rajeev Kumar Singh
17/3/25

Signature of Head of the Department

आचार्य एवं विभागाध्यक्ष / PROFESSOR & HEAD
विद्युत् अभियंता विभाग / Department of Electrical Engineering
भारतीय प्रौद्योगिकी संस्थान / Indian Institute of Technology
(काशी हिन्दू विश्वविद्यालय) / (Banaras Hindu University)
Varanasi, U.P. (INDIA)

COPYRIGHT TRANSFER CERTIFICATE

Title of the Thesis: Soft-Switching Modulation Techniques for Bidirectional Dual Active Bridge Converter Based Battery Charging Systems

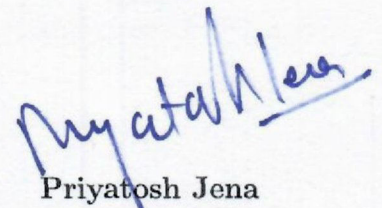
Name of the Student: Priyatosh Jena

Copyright Transfer

The undersigned hereby assigns to the Indian Institute of Technology (Banaras Hindu University), Varanasi all rights under copyright that may exist in and for the above thesis submitted for the award of the *Doctor of Philosophy*.

Date: 17-3-25

Place: Varanasi



Priyatosh Jena

Note: However, the author may reproduce or authorize others to reproduce material extracted verbatim from the thesis or derivative of the thesis for author's personal use provided that the source and the Institute's copyright notice are indicated.

**This thesis is dedicated to Lord Hanuman and to my uncle Sri Yudhisthira
Jena.**

ACKNOWLEDGEMENT

At the outset, I would express my deepest gratitude and abject surrender to Lord Hanuman for his grace of bestowing upon me the strength, courage, wisdom and perseverance to embark on the job of writing this thesis. My uncle, Sri Yudhisthira Jena, in whom I see Lord Hanuman's unwavering dedication, strength, and wisdom has guided me throughout my academic journey, his encouragement has been invaluable and continuously fueled my drive. His unshakeable belief in my abilities has played an important role in my success, and I am profoundly grateful for his constant support.

Besides, and most importantly, I would like to express my deepest gratitude to Prof. Rajeev Kumar Singh and Prof. Vivek Nandan Lal, who have been more than just mentors playing the role of friends, philosophers, and guides. Their unwavering support, insightful advice, and profound wisdom have been instrumental in shaping my research journey. From the very inception of this project, they have not only helped me in navigating every challenge with ease but have also inspired me in expanding the boundaries of my knowledge. Their patience, encouragement, and belief in my potential have been invaluable, and I am truly privileged to have their guidance throughout this endeavour.

Additionally, I would like to express my heartfelt gratitude to Prof. Rajeev Kumar Singh, Prof. Vivek Nandan Lal, and Prof. Ranjit Mahanty, along with their respective families, for their unwavering support and guidance throughout my academic journey. Their insightful advice, constant encouragement, and dedication to my growth have been invaluable in helping me navigate the challenges of this work. Their mentorship has been crucial in shaping both my academic and personal development, and I am truly thankful for their instrumental roles in my success. They have been incredible role models who have taught me the importance of integrity, perseverance, and intellectual curiosity in research. They not only built my academic career but also expertly prepared me for future professional challenges, training me in essential skills for navigating official work and administrative responsibilities. The warm and supportive environment they

and their families created made this challenging journey not just bearable, but truly enriching and memorable.

I would also like to extend my heartfelt thanks to Prof. Sanjay Kumar Singh (CSE, IIT (BHU)) for his invaluable support as an external advisor. His expertise and constructive feedback have significantly contributed to the development of this thesis, and I am deeply grateful for his insights, which have greatly enhanced the quality of my work. My sincere gratitude extends to Prof. Devender Singh, former Head of the Department of Electrical Engineering and current Dean (Academic Affairs), for his constant support throughout this journey. I am especially thankful to Dr. Soumya Ranjan Meher, who has been more than just a senior he has been a brother and a true friend. His invaluable guidance and support during the early stages of my Ph.D. career have been transformative. Without his encouragement and mentorship, I would not have had the opportunity to pursue my Ph.D. at IIT BHU or achieve the milestones I have reached today. His contributions have been instrumental in laying a strong foundation for both my academic journey and personal growth.

I am also deeply grateful to my parents, Ashutosh Jena and Usha Mani Jena, for their endless sacrifices and unwavering belief in me, which have been a constant source of strength throughout my journey. A special thanks to my wife, Smrutirekha Mallick, for her constant motivation and support, which have been crucial to my progress.

I would like to extend my sincere appreciation to Dipak Dnyaneshwar Sonawane and Surakshit Kumar, whose collaboration and support during the formative stages of my research proved invaluable. Their dedicated efforts, insightful contributions, and unwavering commitment were instrumental in laying the foundation and shaping the direction of this work. Their partnership not only enhanced the quality of the research but also made the journey more enriching.

I extend my heartfelt thanks to my friends and colleagues Chandra Pratap Singh, Simanta Kumar Samal, Pawan Kumar, Abhinandan Routray, Manash Kumar Mishra, Somenath Banerjee, Warda Matin Khan, Prakash Ji Baranwal, Rajat Kumar Keshari, Virendra Maurya, Arya Singh, Anantha Padmanabhan N K, Ankit Kumar Pratihasta, Manish Kumar, Aman Kumar, Manoj Arya, Utkarsh Baranwal, Dharmendra Kumar

Yadav, Sudeep Mohaney, Sagar Yadav, Suresh Kumar Pal, Vijay Singh, Ritesh Sharma, Jayashankara M, Vishakha Singh, Dilip Kumar Patel, Dev Singh, Sri Radhe Shyam Patel, Sri Umesh Mishra and Mohammad Vasim. Their direct or indirect support and cooperation have been invaluable in completing this Ph.D. research. I am deeply grateful for their assistance, encouragement, and camaraderie throughout this journey. I also acknowledge those whose names I may have inadvertently missed but whose contributions have been equally significant.

Lastly, I would like to thank the Department of Science and Technology, Ministry of Science and Technology, Government of India, for supporting a part of my work under Sanction Order No. DST/TMD/CERI/RES/2020/6(G) and DST/CERI/MISG/2017/086(IIT(BHU)), Varanasi (G). I am also grateful to the Anusandhan National Research Foundation (ANRF) for providing international travel support to attend ECCE 2024 in Phoenix, Arizona, USA. Furthermore, I extend my gratitude to the Indian Institute of Technology (BHU) for partially funding my participation in IECON 2023, Singapore, ITEC India 2023, Chennai, and PEDES 2024, Surathkal, Mangalore.

Contents

Abstract	xvi
List of Figures	xxi
List of Tables	xxvii
List of Abbreviations	xxix
List of Symbols	xxxii
1 Introduction	1
1.1 Background	1
1.2 Research Motivation	5
1.3 Literature Survey	8
1.3.1 Bidirectional AC-DC DAB Converters	10
1.3.2 Fundamentals of Soft Switching	21
1.3.3 Modulation Techniques	27
1.4 Research Gap and Challenges with Existing Literature	34
1.5 Objective of the Thesis	38
1.6 Organization of the Thesis	40
1.7 Conclusion	42
2 A Novel Soft-Switched Triangular Modulation for DC-AC Dual Active Bridge	43
2.1 Introduction	43
2.2 Converter Topology and Proposed Modulation Technique	45
2.2.1 Converter Analysis and Operation	46
2.2.2 Modulation Technique Using Method 1	50
2.2.3 Modulation Technique Using Method 2	53

2.3	DSP Based Digital Realization of Proposed Techniques	56
2.3.1	Digital Realization of Method 1	56
2.3.2	Digital Realization of Method 2	57
2.4	Simulation and Experimental Validation	59
2.4.1	Simulation Validation	59
2.4.2	Experimental Validation	61
2.5	Discussion	65
2.5.1	Dynamic Performance	65
2.5.2	Soft Switching Analysis	66
2.5.3	Comparison of the Proposed Method with the Existing Literature	68
2.5.4	Efficiency Comparisons with Other TRM	69
2.6	Conclusion	72
3	Improved Benchmark Performance with Triangular Modulation and Quasi Single-Stage AC-DC DAB	73
3.1	Introduction	73
3.2	Analysis and Operating Principle of Q1S AC-DC DAB	77
3.2.1	Operation of Q1S DAB Using Proposed Technique	81
3.3	Realization and Comparison of Switching Sequence for Q1S DAB . . .	84
3.3.1	Realization of Conventional TRM	84
3.3.2	Realization of Proposed TRM	86
3.3.3	Comparison Between Conventional and Proposed TRM	87
3.3.4	Benchmark Evaluation of Both TRM	89
3.4	Experimental Validation	90
3.4.1	Validation of AC→DC Power Flow	91
3.4.2	Status of Various Devices at Different Values of γ	93
3.4.3	Validation of DC→AC Power Flow	93
3.4.4	Dynamic Characteristics of the Proposed System	95
3.4.5	Analysis of THD and Other Power Quality	95
3.5	Comparison With Other Literature	97
3.5.1	Efficiency Comparison	97
3.5.2	Total Harmonics Distortion Comparison	97
3.6	Conclusion	99
4	Asymmetric Semi-Variable Frequency Based Triangular Modulation with Improving Light-Load Performance	101
4.1	Introduction	101

4.2	Mathematical Modeling and the Proposed TRM	104
4.2.1	Mathematical Modeling of the Proposed ASVF TRM	104
4.2.2	Relationship of ζ and f_s with RMS Inductor current	108
4.2.3	Relationship Between THD and Switching Frequency	109
4.2.4	Optimizing ζ and f_s in the Proposed ASVF TRM	110
4.3	Open Loop Control Realization	110
4.3.1	Open Loop Control Realization	110
4.3.2	Converter Design	115
4.4	Experimental Results	118
4.4.1	Steady State Result at Rated Power	118
4.4.2	Soft Switching Performance Analysis	119
4.4.3	Performance of Conventional and Proposed TRMs at Light Load	122
4.4.4	Dynamic Performance at Semi-Variable Frequencies	123
4.4.5	THD and Other Power Quality Indices	125
4.5	Discussion and Comparison	125
4.5.1	Discussion on RMS Current and Conduction Loss	125
4.5.2	Losses Distribution	126
4.5.3	Experimental Efficiency and THD Comparison	128
4.5.4	Comparison with Other Literature	129
4.6	Conclusion	131
5	Hybrid Energy Input-Based DC Charging System	133
5.1	Introduction	133
5.2	Proposed EV Charging System	138
5.3	Proposed Adaptive Optimal Power Management Scheme	141
5.3.1	MPPT with power constraint and voltage controller for boost converter	141
5.3.2	Controller with power factor correction and voltage controller for 3ϕ converter	143
5.3.3	CC-CV charge controller for DAB	145
5.4	Experimental Validation	145
5.4.1	Dynamic variation of PV during mode 2 operation	146
5.4.2	Dynamic variation from mode 2 to mode 3 and vice versa	148
5.4.3	Dynamic load variation	150
5.4.4	Dynamic variation from mode 1 to mode 2 and vice versa	151
5.4.5	Mode 6:- Vehicle to vehicle charging	152

5.4.6	THD of the grid current during mode 3 operation	152
5.5	Comparison with other Charging Systems	152
5.6	Challenges and Future Direction	154
5.7	Conclusion	154
6	Conclusion and Future Directions	157
6.1	Introduction	157
6.2	Conclusion	159
6.3	Future Directions	163
	Appendix A: Loss Calculation	165
A.1	IGBT Conduction Loss	165
A.2	MOSFET Conduction and Switching loss	165
A.3	Gate loss of the Devices	166
A.4	Power Losses in Magnetic Components	166
A.5	Power Losses in Capacitor	167
	Bibliography	169
	List of Publications	191

Abstract

In the rapidly advancing domain of energy storage and power electronics, soft-switching converters have risen as transformative technologies, redefining the future of battery charging systems across diverse applications. These innovative power conversion solutions herald a new era in energy management, delivering unmatched efficiency, reliability, and precision. From powering portable electronic devices to enabling robust charging infrastructure for electric vehicles and renewable energy storage, soft-switching converters embody a leap forward in engineering. By harmonizing state-of-the-art performance with sustainable design, they lay the foundation for a smarter, more eco-friendly energy ecosystem, setting new benchmarks for the future of energy systems.

The core significance of soft-switching converters lies in their remarkable ability to mitigate switching losses, a persistent challenge in traditional hard-switching power conversion methods. In conventional power electronic systems, semiconductor switches endure considerable energy losses during the transition between on and off states, leading to heat generation and reduced system efficiency. Soft-switching converters overcome this limitation through advanced switching techniques that significantly reduce instantaneous power dissipation during these transitions. As a result, they enable substantially higher energy conversion efficiency, making them a pivotal innovation in modern power electronics.

A key innovation in this area is the bidirectional converter, which seamlessly integrates soft-switching with bidirectional power flow capabilities. This converter is crucial for applications that demand efficient energy storage and retrieval, such as electric vehicle battery charging and renewable energy storage. It enables smooth energy transfer for both charging and discharging, effectively managing power between the AC grid and the battery. By leveraging soft-switching techniques, the converter minimizes switching losses during both charging and regeneration, significantly enhancing efficiency and extending the lifespan of components. This makes it a perfect solution for next-generation energy systems requiring efficient power cycling. Specifically, the AC-DC Bidirectional Dual Active Bridge (DAB) converter further amplifies these benefits, optimizing power

conversion with enhanced efficiency, reliability, and flexibility transforming the way energy systems perform and evolve. Advanced modulation techniques play a crucial role in achieving these enhancements, enabling precise control and superior performance.

However, while these advanced modulation techniques significantly enhance the features and performance of the AC-DC bidirectional DAB converter, they also introduce added complexity at the microcontroller implementation level, such as managing a large number of control variables, utilizing multiple carriers, non-linear power relationship, necessitate close-loop to achieve power factor correction and requiring extensive analytical calculations, all of which lead to higher computational costs. This research addresses a critical gap in the literature that often overlooks minimizing computational burden a key factor in enabling the design of custom microcontrollers with lower resource requirements and reduced costs. By tackling this challenge, the study aims to strike an optimal balance between performance and practicality, paving the way for efficient and cost-effective solutions in modern power electronics systems.

To address these research gaps, an innovative triangular modulation technique (TRM) for a DC-AC bidirectional matrix-type DAB converter that overcomes challenges such as the need for multiple control variables, dependence on multiple carriers, and the complexities of non-linear power relationships, which often require closed-loop control to achieve power factor correction. The proposed method employs a sinusoidally modified variable frequency PWM, also known as an asymmetrical switching sequence, to modulate one leg of the H-bridge. This enables true soft-switching by precisely shaping the transformer current and controlling the transformer voltage. The technique simplifies implementation by utilizing a single carrier and is demonstrated digitally on the F28335 MCU, presenting its practicality and efficiency. By eliminating the reliance on complex analytical calculations, the TRM enhances performance and ensures soft-switching across the entire operating range of the converter while maintaining an open-loop power factor. Experimental validation of Method 1, tested at a power level of 500 W for the DC-AC bidirectional DAB converter, highlights its effectiveness in vehicle-to-grid (V2G) and grid-to-home (G2H) applications.

The application of the proposed TRM technique is further investigated for a distinct topology, specifically a 500 W prototype of Quasi Single Stage (Q1S) bidirectional AC-DC DAB converter with an intermediate capacitor. This exploration emphasizes maintaining performance while significantly reducing computational complexity further. By employing an asymmetrical switching sequence-based TRM, the study highlights how minimizing the number of distinct PWM signals can simplify control strategies. The approach stresses the importance of aligning modulation techniques with the

chosen topology to optimize control performance and achieve enhanced benchmarks. Implemented on the Texas Instruments TMS320F28335 microcontroller, this method demonstrates its capability to improve efficiency without compromising essential factors such as soft-switching performance and power quality, further setting a new benchmark in modulation design.

Another key challenge addressed in this research pertains to the high RMS current that leads to increased conduction losses, particularly under light load conditions, which affects both the proposed TRM and other existing TRM modulation techniques. While the phase-shift ratio exhibits a linear relationship with power transfer, the RMS current decreases non-linearly as the phase-shift ratio is reduced to supply power at light loads. This non-linear reduction in current results in higher conduction losses in relation to the output power, negatively impacting overall converter efficiency, especially in battery charging applications. Despite successfully achieving soft-switching during both turn-on and turn-off operations, the TRM modulation scheme still suffers from reduced efficiency at light loads due to these non-linear conduction losses. This work investigates these challenges in detail and explores effective solutions, proposing an improved Method 1 to enhance performance under light load conditions and mitigate these losses using a 500W prototype of Quasi Single Stage (QS^2) bidirectional AC-DC DAB without an intermediate capacitor. Additionally, the proposed modulation significantly reduces total harmonic distortion and current stress at light loads, ensuring better performance.

This research further explores the DC charging system, featuring an innovative adaptive optimal power management scheme for a hybrid energy input-based DC charging setup. This scheme efficiently integrates different energy sources, optimizing power distribution to significantly enhance system efficiency and overall performance. A key highlight is its capability to optimize photovoltaic (PV) power, reducing grid power consumption while ensuring seamless transitions between various modes without disrupting load demand. Additionally, the system supports DC fast charging for Erickshaw batteries, providing rapid dynamic control and high-quality power. This idea is verified on a technology readiness level -6 prototype with a peak rating of 10 KVA.

These works offer an innovative approach to power conversion and energy management, focusing on TRM techniques for bidirectional DC-AC DAB converters, optimizing computational complexity, TRMs realization and enhancing soft-switching performance. They also highlight the integration of adaptive power management in DC charging systems, optimizing photovoltaic power, and improving efficiency in light-load conditions. With a focus on system efficiency, power factor optimization, and renewable energy integration, this research provides key insights into the future of power electronics.

List of Figures

1.1	Life cycle emission of Battery Electric Vehicle, Hybrid Electric Vehicle, and Internal Combustion Engine Vehicle.	2
1.2	India's EV penetration till October 2024. (Source: Vahan Dashboard via clean mobility shift)	3
1.3	Typical operating modes of an EV in V2G, G2V, and V2H scenarios. . .	6
1.4	Bidirectional AC-DC Matrix Type Dual Active Bridge Converter. . . .	12
1.5	Bidirectional Quasi Single Stage (Q1S) AC-DC Dual Active Bridge Converter with Intermediate Film Capacitor.	14
1.6	Bidirectional Quasi Single Stage (QS ²) AC-DC Dual Active Bridge Converter without Intermediate Film Capacitor.	15
1.7	Bidirectional AC-DC Indirect Matrix Type Dual Active Bridge Converter.	16
1.8	Other AC-DC DAB based topologies; (a) Push-pull DAB Topology 1. (b) Multiphase Boost Type DAB Topology 2. (c) Reconfigured AC-DC DAB Topology 3. (d) Current Source DAB Topology 4. (e) Interleaved Inversely Coupled Inductor DAB Topology 5. (e) Single-Phase Boost Type DAB Topology 5.	18
1.9	Switching waveform of device (a). Hard Switching. (b). True and pseudo ZVS (c). True and pseudo ZCS.	23
1.10	Zero voltage transition of MOSFET Leg (a). Free-wheeling state ($i_L=I_1$). (b). Device S_2 turns off, and the resonant transition starts with the additional current path through the DC source during the dead time between two pulses (c). End of transition when the drain-source voltage of S_2 has reached the source voltage. (d). Waveform of various voltages and currents during all three states.	24

1.11	Zero current transition of IGBT Bridge (a). Current path during positive half cycle resulting in ZCS turn ON of S_1 . (b). Current path during positive half cycle resulting in ZCS turn OFF of S_1 (c). Waveform of various voltages and currents during all three states.	26
1.12	Categorization of various modulation techniques for AC-DC DAB with waveforms and their power relationship with control variables.	29
1.13	Asymmetric Modulation Strategies shown for one cycle of switching frequency. (a).Asymmetric TZM. (b). Asymmetric TZM+TRM.	34
1.14	Contributions of the Chapters	42
2.1	Topology of single-phase single-stage matrix-type bidirectional DC to AC dual active bridge converter with high-frequency AC link.	46
2.2	Principle operating waveform of bidirectional DC to AC dual active bridge converter.	48
2.3	Switching sequence and principal operating waveform using method 1.	51
2.4	Various operating modes of the proposed modulation technique over half switching cycle of the converter using method 1 ($v_{ac} > 0$ and $i_{ac} > 0$). (a). Mode 1 ($t_0 \leq t < t_1$), (b). Mode 2 ($t_1 \leq t < t_2$), (c). Mode 3 ($t_2 \leq t < t_3$) and (d). Mode 4 ($t_3 \leq t < t_4$).	52
2.5	Switching sequence and principal operating waveform using method 2.	54
2.6	Various operating modes of the proposed modulation technique over half switching cycle of the converter using method 2 ($v_{ac} > 0$ and $i_{ac} > 0$). (a). Mode 1 ($t_0 \leq t < t_1$), (b). Mode 2 ($t_1 \leq t < t_2$), (c). Mode 3 ($t_2 \leq t < t_3$) and (d). Mode 4 ($t_3 \leq t < t_3'$) (e). Mode 5 ($t_3' \leq t < t_4$).	55
2.7	DSP-based digital realization of method 1 and gating signals of various switches.	57
2.8	Pictorial representation of DSP-based digital realization bidirectional power flow using proposed modulation technique using method 1. (a) DC to AC power Flow and (b) AC to DC power flow.	58
2.9	DSP-based digital realization of method 2 and gating signals of various switches.	58
2.10	Simulation results using method 1; (a) Gating pulses to the primary bridge. (b) Input, output voltages, and currents for DC-AC power flow. (c) Transformer voltages and currents. (d) Zoomed view of Fig. 12(c). (e) Input, output voltages, and currents for AC-DC power flow. (e) Zoomed view of transformer voltages and current for DC-AC power flow.	60

2.11	Experimental prototype of single-phase single-stage bidirectional DC to AC dual active bridge converter.	62
2.12	Experimental results showing (a) Gate pulses for the various switches. (b) Zoomed view of the (a) near zero crossing of v_{ac} . (c) Gate pulses for the DC side bridges when power is delivered from the DC to the AC side. (d) Showing V_{dc} , v_p , v_s , and i_{Lk} , for two cycles of line frequency. (e) Zoomed view of Fig. 14(d). (f) Showing v_{ac} , i_{ac} , I_{dc} and V_{dc} . (g) Showing i_{ac} , v_{ac} , V_{dc} , and v_s for AC to DC power flow. (h) Showing v_s , v_p , and i_{Lk} when power is delivered from AC to DC side. (i) Showing input v_{ac} , i_{ac} , I_{dc} and V_{dc} . (j) THD of i_{ac} during AC to DC power flow.	63
2.13	Dynamic performance under 51% step change in the load. (a) Showing dynamics variation from 500 W to 248 W. (b) Showing transformer voltages and current before dynamics. (c) Showing transformer voltages and current after dynamics.	65
2.14	Simulation and experimental results of soft switching. (a) simulation and (b) experimental results of ZVS turn ON of DC side switch $Q1$. (c) simulation and (d) experimental results of ZCS turn OFF of DC side switch $Q1$. (e) simulation and (f) experimental results of ZCS turn ON of DC side switch $Q3$. (g) simulation and (h) experimental results of ZCS turn OFF and ZVS Turn ON of DC side switch $Q3$. (i) simulation and (j) experimental results of ZCS turn ON of AC side switch $Q1a$. (k) simulation and (l) experimental results of ZCS turn OFF of AC side switch $Q1a$	67
2.15	Efficiency comparison between conventional and the proposed modulation technique	71
3.1	Switching sequence of the Matrix-type AC-DC DAB Converter showing zoomed in view near the grid voltage zero crossing: (a) Conventional (b) Proposed TRM.	75
3.2	Switching sequence of the Q1S AC-DC DAB Converter showing zoomed in view near the grid voltage zero crossing (a) Conventional (b) Proposed TRM.	76
3.3	Schematic diagram of Q1S AC-DC bidirectional DAB converter.	78
3.4	Key operating waveform of proposed TRM.	79
3.5	Plot showing soft switching region (a). Average power in per unit (\bar{P}_{PU}) as a function of \hat{k} and γ (b). Front view showing $\bar{P}_{PU} \sim \gamma$	82

3.6	Equivalent circuits of the Q1S DAB using proposed modulation technique (a). Mode 1 $[t_0 - t_1]$. (b). Mode 2 $[t_1 - t_2]$. (c). Mode 3 $[t_2 - t_3]$. (d). Mode 4 $[t_3 - t_4]$	83
3.7	Block diagram representation of switching sequence for the conventional TRM	85
3.8	Switching sequence of the conventional TRM.	86
3.9	(a) Proposed switching sequence using a single carrier. (b) Overall control block diagram.	87
3.10	Status of devices. (a) Primary side device Q_1 status using both TRM. (b) Secondary side device Q_5 status using a conventional TRM. (c) Secondary side device Q_5 status at a fixed time period using the proposed TRM. (d) Secondary side device Q_7 status at a variable time period using the proposed TRM.	88
3.11	Experimental prototype of bidirectional Q1S DAB with asymmetrical full bridge.	90
3.12	(a) Gate pulses for the various devices. (b) v_g , v_p , I_{dc} , i_g , and p_g . (c) v_x , v_p , \bar{i}_{ac} , and Ni_{Lk} . (d) v_x , v_p , \bar{i}_{dc} , and Ni_{Lk}	92
3.13	(a) Magnified view of v_x , v_p , \bar{i}_{ac} , and Ni_{Lk} near peak of v_g . (b) Magnified view of v_x , v_p , \bar{i}_{dc} , and Ni_{Lk} near peak of v_g	93
3.14	Transformer voltages and current at different γ (a) v_p , v_x , and Ni_{Lk} at γ $= 10^\circ$. (b) v_p , v_x , and Ni_{Lk} at $\gamma = 20^\circ$. (c) v_p , v_x , and Ni_{Lk} at $\gamma = 32^\circ$. d). v_x , v_p and Ni_{Lk} near zero crossing.	94
3.15	(a) v_g , i_g , v_p , and v_x . (b) Magnified view of v_x , v_p , and Ni_{Lk}	94
3.16	Dynamic response for a step change in load from 487 W to 270 W.	95
3.17	(a) Experimental THD of i_g up to 100 th harmonics. (b) Various power quality parameters.	96
3.18	Comparison plot showing (a) Efficiency versus power plot (b) THD versus power plot.	98
4.1	Different types of TRM based on DC side H-bridge modulation.	102
4.2	Topology of the bidirectional QS ² AC-DC DAB converter without intermediate capacitor.	104
4.3	Operation waveform of the proposed ASVF TRM.	105
4.4	Input current to DAB (i_{sr}) and the fundamental component of i_g (I_1) shown for one and half cycle of AC.	109
4.5	The mechanism for generating switching sequences for high-frequency devices using a lookup table for the proposed ASVF TRM.	112

4.6	Experimental prototype of the bidirectional QS ² AC-DC DAB converter.	119
4.7	Gate pulses for device Q_1 and Q_7 .	120
4.8	Experimental results showing (a) v_s, v_g, v_p, i_g and p_g (b) i_g, v_g, I_{bat}, v_s and p_g . (c) v_s, v_g, v_p , and i_o . (d) v_s, v_g, v_p , and i_i .	120
4.9	Soft switching performance of the various devices. (a) Magnified view of v_s, v_g, v_p , and i_{Lk} . (b) Magnified view of v_s, v_p, i_o , and i_{sr} .	121
4.10	Performance of conventional and proposed TRMs at 27% (a). Conventional TRM showing v_p, v_s, I_{bat} , and i_{Lk} . (b) Zoomed view of (a) at $f_s=10$ kHz and $\zeta = 10^\circ$. (c) Proposed TRM showing v_p, v_s, I_{bat} , and i_{Lk} (d) Zoomed view of (c) at $f_s \approx 30$ kHz and $\zeta \approx 27^\circ$.	123
4.11	Dynamic performance under light load condition. (a). Dynamic performance in charging mode. (b) Dynamic performance in discharging mode. (c) Steady-state operation at 15 kHz. (d) Steady-state operation at 18 kHz.	124
4.12	Power quality parameters. (a). THD of grid current i_g . (b) Other power quality indices.	126
4.13	Variation of $i_{Lk,rms}, i_{Lk}(t_1)$, and I_{bat} with ζ/f_s .	127
4.14	Loss comparison at 27% load: Conventional vs. Proposed TRM	127
4.15	Comparison between conventional and proposed TRM (a). Efficiency comparison. (b) THD comparison.	128
4.16	THD at 17% of the rated load.	129
5.1	Electric three-wheelers sales per year till 2030. (Source: EV Vahan Dashboard by cleanmobilityshift.com)	134
5.2	Various E-3W models available in India.	136
5.3	(a) Block diagram of the proposed EV charging system with AOPM scheme. (b) Circuit diagram.	139
5.4	Flowchart of proposed adaptive optimal power management scheme.	142
5.5	Control logic of various controllers. (a) MPPT with power constrain and voltage controller. (b) Controller with power factor correction and voltage controller. (c) CC-CV charge controller.	144
5.6	Experimental prototype of the E-rickshaw charging system.	147
5.7	PV characteristics at STC.	147
5.8	Photograph of pylontech make US2000 lithium battery as ③.	147

5.9	Dynamic variation of PV during mode 2 operation. (a) source characteristics during dynamic variation of solar irradiance from $500 \text{ W/m}^2 \rightarrow 1000 \text{ W/m}^2 \rightarrow 800 \text{ W/m}^2$. (b) Magnified view of irradiance change from 500 W/m^2 to 1000 W/m^2 . (c) Magnified view of irradiance change from 1000 W/m^2 to 800 W/m^2 . (d) Reflection of dynamics in the DC-Link and RESS ③. (e) CV charging of the battery (RESS) ③.	149
5.10	Dynamic variation from mode 2 to mode 3 and vice versa. (a) mode variation from 3 to 2. (b) mode variation from 2 to 3.	150
5.11	Dynamic variation in load by 50%. (a) A step decrease in load. (b) A step increase in load.	150
5.12	Dynamic variation from mode 2 to mode 1 and vice versa. (a) mode transition from 2 to 1. (b) mode transition from 1 to 2.	151
5.13	Vehicle-to-vehicle charging. (a) voltages and currents DAB connected with RESS ③. (b) DAB voltages and current connected EV_1	152
5.14	THD of the grid current of phase A.	153

List of Tables

2.1	Power Delivered by the Converter During Various Time Intervals	50
2.2	Status of the Switches During Transition In DC to AC Power Flow Using Method 1.	54
2.3	Status of the Switches During Transition in DC to AC Power Flow Using Method 2.	56
2.4	Design Parameters	61
2.5	Component Selected	62
2.6	Comparison with Various Modulation Techniques	70
2.7	Efficiency comparison with the proposed and existing TRM	71
3.1	Summary and Comparison with Various Converter Typologies and Modulation Techniques	76
3.2	Comparison between the status of devices	89
3.3	Specifications of Various Components	91
3.4	Comparison of Efficiency and Other Key Parameters	97
3.5	Comparison of THD and Other Key Parameters	99
4.1	Specification of QS ² DAB	112
4.2	Analog and digital equivalents of control parameter	113
4.3	Comparison with Other Works	130
5.1	Specifications of the Various Converter Components	146
5.2	Comparison of Various EV Charging Systems	153

List of Abbreviations

Abbreviation	Description
ADC	Analogue to Digital Conversion
ASVF	Asymmetrical Semi-Variable Frequency
C2C	Center-to-Center
CC	Constant Current
CMPA	Compare A
CMPB	Compare B
CT	Circuit Topology
CV	Constant Voltage
DAB	Dual Active Bridge
DoF	Degree of Freedom
DPS	Dual-Phase Shift
DSP	Digital Signal Processor
EMC	Electromagnetic Compatibility
EMI	Electromagnetic Interference
EPS	Extended-Phase Shift
EPWM	Enhanced Pulse width Modulator
EV	Electric Vehicle
FPGA	Field Programmable Gate Array
G2V	Grid-to-Vehicle

Abbreviation	Description
HF	High-Frequency
IGBT	Insulated-Gate Bipolar Transistor
MCUs	Micro controller Units
MOSFET	Metal-Oxide-Semiconductor Field-Effect Transistor
PF	Power Factor
PFC	Power Factor Correction
PWM	Pulse Width Modulation
Q1S	Quasi Single-Stage DAB (with intermediate capacitor)
QS ²	Quasi Single-Stage DAB (without intermediate capacitor)
RES	Renewable Energy System
RESS	Renewable Energy Storage System
RMS	Root Mean Square
SPS	Single Phase Shift
SR	Synchronous Rectifier
TBCLK	Time-Base Clock
TBPRD	Time-Base Period
THD	Total Harmonics Distortion
TPS	Triple-Phase Shift
TRM	Triangular Modulation
TZM	Trapezoidal Modulation
UPF	Unity Power Factor
V2G	Vehicle-to-Grid
V2H	Vehicle-to-Home
ZCS	Zero Current Switching
ZVS	Zero Voltage Switching

List of Symbols

Symbol	Description
A_e	Effective Area of Core
A_L	Inductance Factor
A_w	Cross Section Area of Core
α, γ and ζ	Phase Shift Ratio
B_{max}	Peak Magnetic Flux Density
C_{ac} and C_g	AC Grid Side Capacitor
C_{bat}	Battery Side Capacitor
C_{dc}	DC Side Capacitor
Δt	Phase shift measure from center-to-center of v_p and v_s
δ	Dissipation Factor of the Dielectric Material
$d(t), k(t)$ and $m(t)$	Duty Ratio
\hat{d}, \hat{k} and \hat{m}	Peak Value of Duty Ratio
E_{OFF}	Device Turn-OFF Energy Loss
E_{ON}	Device Turn-On Energy Loss
f_g	Grid Frequency
f_s	Switching Frequency
\bar{i}_{ac}	Average Grid Current Measured Over Switching Frequency
i_c	Collector Current
i_g and i_{ac}	AC Grid Current

Symbol	Description
I_{bat}	Battery Current
I_{dc}	DC Bus Current
$I_{m,rms}$	Current through Magnetic Component
I_{out}	Output Current
i_{Lk}	Current Flowing through Leakage Inductance
$i_{Lk,rms}$	RMS Value of i_{Lk} Measured Over Grid Frequency
$\langle i_{Lk,rms} \rangle$	RMS Value of i_{Lk} Measured Over Switching Frequency
$i_{Lk}(t_x)$	Current through Leakage Inductance at Different Time Instances
$\tilde{i}_{o,rms}$	Residual Ripple
$i_{i,ripple,rms}$	AC Ripple RMS
J	Current Density
$k, \alpha, \text{ and } \beta$	Steinmetz coefficients
L_{ac}	AC Side Inductor
L_{bat}	Battery Side Inductor
L_{dc}	DC Side Inductor
L_g	AC Grid Side Inductor
L_k	Leakage Inductance of Transformer
L_m	Magnetizing Inductance of Transformer
N	Turns Ratio
$P_{(ON-OFF)}$	Turn On and OFF Loss
$P_{bat,avg}$	Battery Power Measure Over Half of Grid Frequency
P_{copper}	Copper Loss
P_{core}	Core Loss
$P_{cond,IGBT}$	IGBT Conduction Loss
$P_{dielectric}$	Dielectric Loss of the Capacitor
P_{ESR}	Losses due to Equivalent Series Resistance

Symbol	Description
$P_{Loss,gate}$	Power Loss in the Gate of the Device
p_g	Grid Power Measure Over Grid Frequency
$R_{DS(ON)}$	Static On-Resistance of MOSFET
R_{eq}	Equivalent Resistance
R_{mc}	Winding Resistance
T_s	Switching Time
ω_g	Angular Grid Frequency
ω_f	Angular Switching Frequency
V_e	Effective Volume of the Magnetic Components
V_{bat}	Battery Voltage
V_{dc}	DC Bus Voltage
V_{ds}	Drain to Source Voltage of the MOSFET
V_g, V_{ac}	Peak Value Grid Voltage
V_{out}	Output Voltage
$V_{ce(sat)}$	Collector-Emitter Saturation Voltage
v_g, v_{ac}	Grid Voltage
v_{ge}	Gate-to-Emitter Voltage
v_{gs}	Gate-to-Source Voltage
v_p	Transformer Primary Voltage
v_s	Transformer Secondary Voltage
v_x	Transformer Secondary Voltage Reflected to Primary
μ_{eff}	Relative Permeability of a Core
μ_0	Permeability of Free Space

